Scattering and dephasing of excitonic polaritons in CuCl

2002 J. Phys.: Condens. Matter 14 3627

(http://iopscience.iop.org/0953-8984/14/13/319)

INSTITUTE OF PHYSICS PUBLISHING JOURNAL OF PHYSICS: CONDENSED MATTER

J. Phys.: Condens. Matter **14** (2002) 3627–3639 PII: S0953-8984(02)28787-1

Scattering and dephasing of excitonic polaritons in CuCl

E Vanagas[1,2], D Brinkmann[1], J Kudrna[1,3], O Crégut[1], P Gilliot[1], R Tomasiunas[2] and B Hönerlage[1]

[1] Institut de Physique et Chimie des Matériaux de Strasbourg, Groupe d'Optique Non Linéaire et d'Optoélectronique, Unité mixte 7504, CNRS-ULP, 23, rue du Loess, 67037 Strasbourg Cedex 02, France
[2] Institute of Materials Science and Applied Research, Vilnius University, Sauletekio 10, 2040 Vilnius, Lithuania
[3] Department of Chemical Physics, Charles University, Ke Karlovu 3, 12116 Prague 2, Czech Republic

Received 4 September 2001, in final form 4 January 2002
Published 22 March 2002
Online at stacks.iop.org/JPhysCM/14/3627

Abstract

We study the energy and intensity dependence of the dephasing time T_2 of the polarization in CuCl inside an excitonic resonance by a femtosecond four-wave mixing technique at 5 K. We first compare results obtained on bulk material and on epitaxial films of different thicknesses for a backward-scattering configuration. This configuration is most sensitive to the region close to the surface of the samples. In bulk material, the coherence properties of the polarization are mainly limited by recombination processes and scattering with acoustic phonons while they are in addition influenced by scattering with impurities and/or imperfections in the epitaxial films. In these films, in a transmission configuration, the polarization dephases less rapidly than it appears in retrodiffusion, indicating the importance of surface recombination processes and of the polariton propagation.

1. Introduction

Exciton phase relaxation was investigated in a number of quantum confined structures [1–10], using four-wave mixing (FWM) techniques in different configurations. In bulk material, it is mainly the coherence properties of localized states in ternary compounds [11], bound-exciton complexes [12], exciton–biexciton transitions [13], and biexcitons [14, 15] that have been studied. The results obtained have been discussed in terms of localization or scattering of coherent excitons or biexcitons with defects, free carriers, coherent or noncoherent excitons, and phonons.

For free dipole-active excitons in bulk material, where polariton effects become important, the situation is quite different and the energy dependencies of scattering processes, which limit

the coherence times, have been studied [16–20] less extensively. This is partly due to the fact that the absorption of samples close or within their excitonic resonances is very strong. This makes FWM experiments in a transmission configuration quite difficult to perform, and thin samples have to be used. In reflection, on the other hand, surface effects are dominant and the polarization induced by the light field is qualitatively different from that of excitonic polaritons, which are the propagating modes inside the crystal [21]. At the surface, in addition to the bulk modes, surface polaritons exist, which propagate almost parallel to the surface but do not decay radiatively [22]. They can, however, contribute to polariton dephasing due to scattering. In addition, because of the important absorption at the exciton resonance, high-density effects can show up, which complicate the interpretation of the results obtained even more.

As we will discuss in detail, CuCl possesses only a few, well-separated electronic resonances. This simple structure, the significant binding energies of excitons and biexcitons, and the absence of any electron–hole plasma under resonant exciton excitation conditions make CuCl a model semiconductor in which to study electronic excitations close to the absorption band edge. The study of the coherence properties is very attractive since quasiparticles can be excited selectively, even if spectrally broad femtosecond laser sources are used. One should stress, however, that the excitons (and in consequence also the excitonic polaritons) still have an internal degree of freedom. Therefore, their coherence can be destroyed by a simple spin-flip in the exciton wavefunction, which can be induced by elastic scattering processes with defects or with other quasiparticles.

We discuss in this work the influence of the polariton effect on the dynamics of coherent signal generation inside the exciton resonance in bulk CuCl and in thin epitaxial films. We show for a reflection configuration that in bulk CuCl at 5 K, recombination and dephasing processes are enhanced due to surface effects, while in thin films additional scattering with crystal imperfections and/or impurities becomes important. When comparing our results to those obtained with a thin film in a transmission configuration, we can estimate the contributions of surface effects to the dephasing.

2. Optical properties of CuCl

Copper chloride has cubic zinc-blende structure. It is a direct-band-gap semiconductor with an energy gap of about 3.4 eV at 4 K, whose lowest-lying conduction band (transforming like Γ_6) and highest valence band of Γ_7 symmetry are only spin degenerate. The next valence band, of Γ_8 symmetry, is separated from the highest one by 69 meV due to spin–orbit coupling. In this situation, the exciton ground state (the corresponding exciton series is labelled Z_3) is fourfold degenerate with a binding energy of 190 meV at 4 K. The exciton states transform as Γ_2 and Γ_5, respectively. As a consequence of the significant binding energy, the exciton Bohr radius is very small (about 0.7 nm). The analytical and the nonanalytical exchange interactions lift the degeneracy of the ground state. It is thus split into a triplet exciton state ($E_{tr} = 3.2000$ eV), twofold-degenerate transverse excitons, and a longitudinal exciton [21]. Since the transverse excitons are dipole active, they couple strongly to the light field and form new quasiparticles: the excitonic polaritons. In the 'bottleneck region' of these polaritons (situated roughly between the energy of the transverse exciton at $E_T = 3.2025$ eV and that of the longitudinal exciton at $E_L = 3.2080$ eV [23]) their dispersion relation $E(\boldsymbol{k})$ (where E is the energy of the polariton and $\boldsymbol{k}$ its wavevector) is almost horizontal. This gives rise to a very small group velocity v_g and a high density of states of the polaritons in the bottleneck region. In addition, the polaritons are exciton-like and can undergo scattering processes. It is important to notice that exciton states of a given wavevector contribute to both the upper- and lower-branch polaritons. Because of this coupling, the dephasing of excitonic polaritons inside the

bottleneck region will reflect the dephasing of the upper-branch polaritons equally as well as that on the lower branch. In addition, excitonic molecules (or biexcitons) have been identified in CuCl by means of two-photon absorption [24, 25]. Their binding energy (measured with respect to the energy of two triplet excitons $2E_{tr}$) is also very significant (28 meV).

3. Samples and experiment

FWM experiments were performed on CuCl samples of different types: monocrystalline CuCl platelets were grown by a vapour-phase transport method in a closed tube containing H_2 and CuCl powder [26]. The thickness of the platelets studied here in detail is about 20 μm. Epitaxial CuCl films with thickness of 3–0.1 μm were grown on cleaved CaF_2 substrates by the thermal evaporation method. The samples are placed in a cryostat, which is equipped with a temperature-controlled helium gas flow and cooled down to 5 K.

We use in our experiments degenerate FWM techniques in a standard two-beam configuration. The spectrally broad femtosecond pulses from a self-mode-locked Ti:sapphire laser are frequency doubled by a beta-BaB_2O_4 (BBO) crystal. The photon energy of the excitation is centred at 3.202 eV ($\lambda_L = 387$ nm). The full width at half-maximum (FWHM) for the frequency-doubled femtosecond pulses (with a duration of $\tau_L = 140$ fs) is about 18 meV (2.2 nm). The beam is split into two parts of equal intensity. These collinearly polarized light beams with wavevectors $\boldsymbol{k}_1$ and $\boldsymbol{k}_2$ are focused onto the surface of the sample. The FWM signal is then detected—time-integrated but spectrally resolved—by a spectrometer and a photomultiplier, using lock-in techniques. The signal is analysed as a function of the time delay Δt between the two incident pulses for various excitation intensities. The backward-scattering (reflection) configuration is chosen since (even when using high-quality samples) the signal is strongly reabsorbed in the exciton spectral region. However, we compare our results with those obtained with our thinnest sample in the forward-scattering (transmission) configuration.

Figure 1 shows the photon energy dependence of the FWM signal intensity in the reflection configuration (full curve) for a delay of 300 fs between the two pulses. The sample is a film of 0.1 μm thickness. It is compared to the spectral shape of the incident laser pulse (dotted curve), and to the spectral shape of the pulse, transmitted through the sample (dashed curve), not corrected for reflection losses. One clearly observes that the FWM signal is centred in the region of high absorption. It has its maximum at 3.206 eV, i.e. inside the bottleneck region, and shows a shoulder at 3.202 eV. The latter energy corresponds to the spectral position of the minimum of the group velocity of excitonic polaritons in CuCl [27].

4. Experimental results in retrodiffusion

Figure 2 shows the spectrally resolved FWM signal intensity as a function of time delay Δt in a semilogarithmic plot for the 0.1 μm film sample. The total-intensity difference between minimum (black) and maximum (white) corresponds to five decades. As in figure 1, the signal is important only in the bottleneck region and its maximum is situated at 3.207 eV and at temporal coincidence. The excitation intensity per pulse is 1.6 MW cm^{-2} (2.5×10^{11} photons cm^{-2}). One clearly observes that the decay dynamics depends on the photon energy of the signal and that with increasing delay time Δt between the two pulses, the maximum of the signal shifts to lower photon energies.

If we analyse the dynamics of the signal, we find that the signals decay exponentially for most photon energies, except for photon energies between 3.199 and 3.202 eV. Figure 3 shows

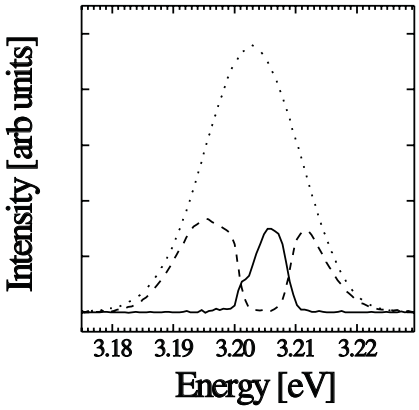

Figure 1. The energy dependence of the FWM signal intensity for a delay $\Delta t = 300$ fs in the reflection configuration (solid curve) and the transmitted intensity of the laser pulse—through the 0.1 μm film sample—not corrected for reflection losses (dashed curve). The spectral shape of the incident pulse is also shown (dotted curve).

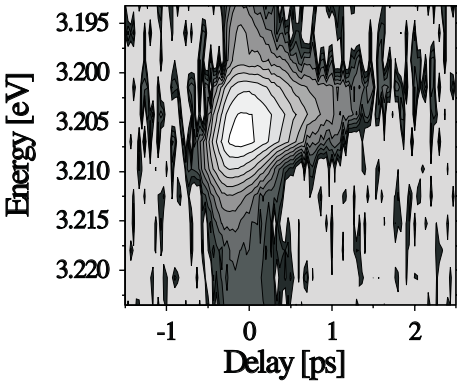

Figure 2. Spectrally resolved FWM signal intensity as a function of the time delay Δt between the pulses in the exciton spectral region for the 0.1 μm CuCl film on CaF_2 substrate in a reflection configuration. Laser pulses (FWHM of 18 meV, 140 fs duration) are centred at the photon energy 3.202 eV. The plot is on a logarithmic scale and five decades are shown.

the signal decrease as a function of Δt for a photon energy of 3.202 eV on a semilogarithmic scale. The signal shows two contributions. We analyse it in terms of a double-exponential decay of the form

$$I = A_1 \exp(-\Delta t/\tau_1) + A_2 \exp(-\Delta t/\tau_2), \tag{1}$$

where τ_1, τ_2 are time constants and A_1, A_2 statistical weights, respectively. The inset of figure 3 gives the different time constants as functions of photon energy. We observe in all cases the fast decay with a time constant of about $\tau_1 = 0.13$ ps and in the region around 3.202 eV a slowing down of the decay to one with a time constant of $\tau_2 = 0.45$ ps. The time constant $\tau_1 = 0.13$ ps is shorter than our time resolution, indicating that the dephasing processes are faster.

We now present FWM measurements on different CuCl samples and for several excitation intensities, i.e. for different exciton densities. The experiments are performed in a reflection configuration. When studying a 20 μm thick CuCl platelet, as shown in figure 4(a) for a

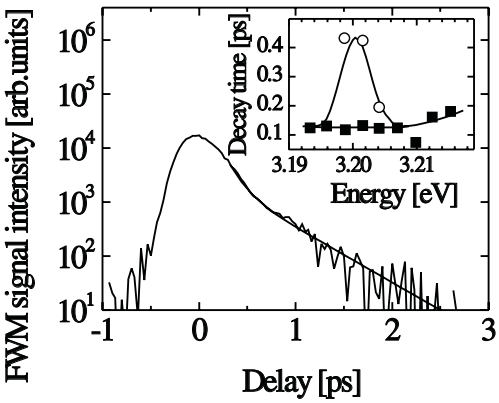

Figure 3. FWM signal intensity as a function of time delay at a photon energy of 3.202 eV in a reflection configuration. The solid curve corresponds to a fit by a double-exponential function. The inset shows the decay time constants as functions of the photon energy in the exciton bottleneck region. Filled squares give the fast part, open circles the slow part.

photon energy of 3.203 eV and a maximum excitation intensity of 0.725 MW cm^{-2}, the signal decrease can again be analysed in terms of a double-exponential decay (equation (1)). The time constants are about $\tau_1 = 130$ fs and $\tau_2 = 600$ fs, respectively. No intensity dependence is observed. The slow decay time constant and the relative intensities of the two contributions depend on the photon energy. This is shown in more detail for the same platelet in figure 4(*b*). Here, the photon energy of detection is tuned to 3.195 eV and the maximum excitation intensity is 1.6 MW cm^{-2}. At this photon energy, we observe only the slow exponential decay of the signal with a time constant of about $\tau = 400$ fs while that of the thin film (see the inset of figure 3) is much faster. The FWM decay dynamics is again independent of the excitation intensity, which can, however, only be varied by a factor of 10.

Close to 3.202 eV, CuCl epitaxial films show a dynamics which is similar to that of bulk material. As shown in figures 4(*c*) and (*d*), where the maximum excitation intensity is again 1.6 MW cm^{-2}, the time constants are about $\tau_1 = 130$ fs and $\tau_2 = 385$ fs, respectively, for the sample of 3 μm thickness, and about $\tau_1 = 150$ fs and $\tau_2 = 480$ fs for the sample of 0.1 μm thickness. As discussed above, the decay times τ_2 are shorter for other photon energies. The τ_2-value given above is slightly higher than the one deduced from figure 3 where the sample was studied under the same conditions as here. This gives an estimate of the error bars (<10%) in our analysis.

Figure 5 shows for the same photon energy (3.202 eV) the values of A_1 and A_2, as a function of exciton density, for the sample of 0.1 μm thickness. As for the platelet, the statistical weight A_1 of the fast component is the most important at this photon energy. The slow part with statistical weight A_2 is much smaller, while it dominates in the platelet for a photon energy of 3.195 eV. It is important to notice that the sums $A_1 + A_2$ usually increase with the exciton density with an exponent between 2 and 3. This indicates that saturation effects are not important, since an exponent 3 is expected for a simple $\chi^{(3)}$-process.

From the fit of the experimental data, we plot in figure 6 the dephasing rates $\Gamma = \hbar/\tau_i$ (where $i = 1, 2$), as a function of the exciton density, for both regions:

$$\Gamma(n_x) = \Gamma_0 + \beta_{IX} n_X, \tag{2}$$

where Γ_0 is the density-independent dephasing rate at 5 K, β_{IX} is the parameter characteristic for polariton–polariton scattering, and n_X the density. As shown in figure 6, in the A_2-region

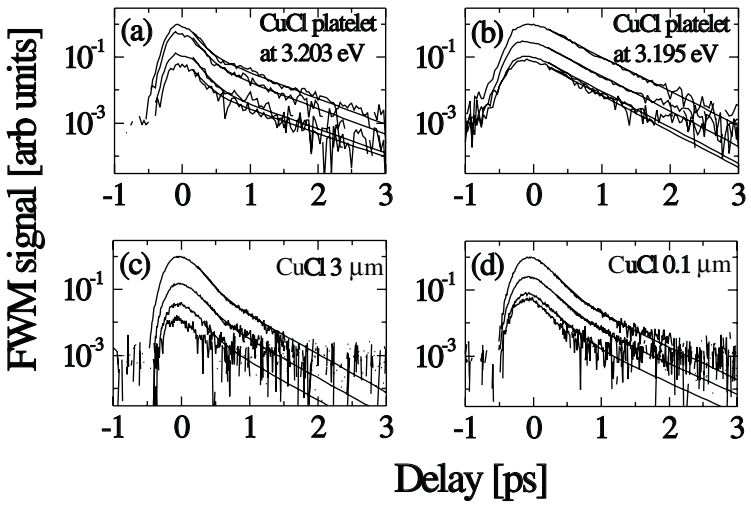

Figure 4. FWM signal intensities versus delay time in a reflection configuration for a CuCl platelet at a photon energy of (*a*) 3.203 eV; (*b*) at 3.195 eV and for CuCl films of (*c*) 3 μm; (*d*) 0.1 μm thickness, close to 3.202 eV photon energy. The maximum excitation intensity for (*a*) is 0.725 MW cm^{-2} (corresponding to the uppermost curve). For each curve below, the excitation intensity is reduced by factors 2, 8, 16, respectively. In (*b*)–(*d*) the maximum intensity is 1.6 MW cm^{-2}, which corresponds to the uppermost curves; for each curve below, the excitation intensity is reduced by a factor of two. Solid curves are double-exponential fits of the experimental data.

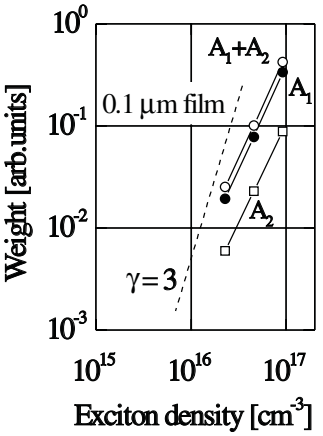

Figure 5. Dependences of the double-exponential decay parameters on the exciton density for the CuCl film with 0.1 μm thickness. A_1 (full circles), A_2 (squares), and $A_1 + A_2$ (open circles) are the statistical weights for the fast and slow parts of the decay and their sum, respectively. An additional eye-guiding dashed line gives the cubic intensity dependence of $\chi^{(3)}$.

the density-independent dephasing rates $\Gamma_0 = 2\hbar/T_2$ are found to be about 1.1 and 1.64 meV for the CuCl platelet when studied at 3.203 and 3.195 eV, respectively. In the A_1-region the dephasing rates Γ_0 differ significantly from one film to the other, showing the extrinsic character of the scattering processes involved. For the polariton–polariton scattering parameter β_{IX}, the numerical fit gives values which are smaller than but of the order of 10^{-20} meV cm^3. As shown in figure 6, the contribution of such scattering to the dephasing is not significant

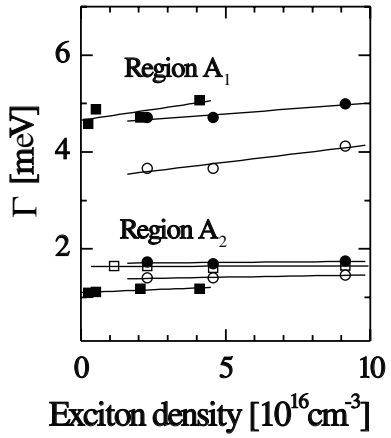

Figure 6. Dephasing rate corresponding to the measured dephasing times versus exciton density. Solid squares represent the dephasing rate in the platelet at a photon energy $E = 3.203$ eV; open squares—rate in the platelet at $E = 3.195$ eV (slow part only); solid circles—rate in the film of 3 μm thickness at $E = 3.202$ eV; open circles—rate in the film of 0.1 μm thickness at $E = 3.202$ eV. All data are obtained for the fast (A_1-region) and slow (A_2-region) parts of the decay. Solid lines show the fit of the experimental points according to equation (2).

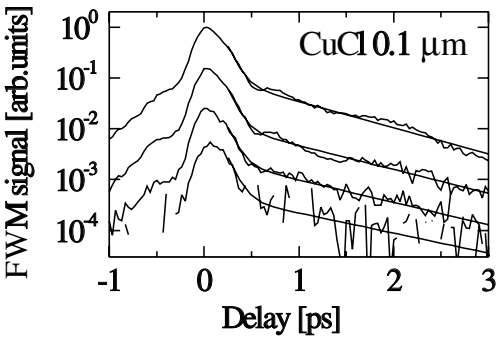

Figure 7. FWM signal intensity as a function of time delay for a CuCl film of 0.1 μm thickness at a photon energy of 3.207 eV in a transmission configuration. The maximum excitation intensity is 0.45 MW cm^{-2} (exciton density 4×10^{15} cm^{-3}) and corresponds to the uppermost curve; for each curve below, the excitation intensity is reduced by a factor of two. Solid curves are double-exponential fits of the experimental data.

in our experiment and the values of β_{IX} obtained are not precise. We therefore consider the dephasing rate Γ to be independent of the polariton density in our experimental conditions.

5. Experimental results in transmission

Figure 7 shows the FWM signal intensity as a function of time delay obtained with the CuCl film of 0.1 μm thickness on a CaF_2 substrate in a transmission configuration for different excitation intensities. This thin film has been chosen [15] in order to have a sufficiently low reabsorption of the signal at the exciton resonance. The maximum intensity is 0.45 MW cm^{-2}. In the transmission configuration, the excitation intensity could be chosen lower than in the reflection case since the signal was much stronger. The central photon energy of the laser is

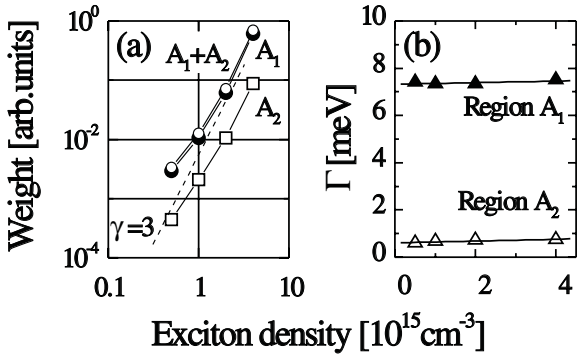

Figure 8. FWM data for the transmission configuration experiment on the CuCl film of 0.1 μm thickness as in figure 7: (*a*) dependences of the double-exponential decay parameters on the exciton density. A_1 (full circles), A_2 (squares), and $A_1 + A_2$ (open circles) are the statistical weights for the fast and slow parts of the decay and their sum, respectively (the eye-guiding dashed line gives the cubic intensity dependence of $\chi^{(3)}$); (*b*) dephasing rate corresponding to the measured dephasing times versus exciton density. The data are obtained for the fast (A_1-region, solid triangles) and slow (A_2 region, open triangles) parts of the decay. Solid lines show the fit of the experimental points according to equation (2).

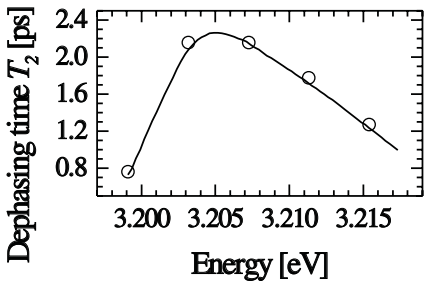

Figure 9. Coherence time T_2 as a function of photon energy for the 0.1 μm CuCl film in a transmission configuration.

at 3.202 eV and the detection is at 3.207 eV. As in the reflection case, the time-integrated, spectrally resolved FWM signal emitted into the direction $\boldsymbol{k}_s = 2\boldsymbol{k}_2 - \boldsymbol{k}_1$ is analysed. Again, a FWM signal is generated in the bottleneck region of the exciton resonance. It is maximal at temporal coincidence of the pulses.

When the time delay between the pulses is increased, the signal intensity diminishes, reflecting the phase relaxation of the polaritons. We can fit the decay as in the reflection configuration by the double-exponential function (equation (1)). The resulting values of A_1 and A_2 as functions of exciton density are given in figure 8(*a*). As shown in detail in figure 7, the signal decays with a time constant of $\tau_1 = 90$ fs for short delays and with a time constant of $\tau_2 \leqslant 1100$ fs for long delay times. Using equation (2), we obtain the density-independent dephasing rate Γ_0 as 0.6 meV at 5 K together with the scattering parameter $\beta_{IX} = 3.7 \times 10^{-20}$ meV cm^3, characteristic for polariton–polariton scattering inside the bulk of the film. As shown in figure 8(*b*), similarly to the case for the reflection configuration, the corresponding decay rates $\Gamma = \hbar/\tau$ do not significantly depend on the excitation intensity.

At temporal coincidence, the maximum of the signal intensity is situated between 3.204 and 3.207 eV, inside the bottleneck region of the polariton dispersion where the density of states

is highest [27]. Unlike the case for the reflection configuration, with increasing time delay the maximum of the FWM signal remains at a fixed spectral position. As discussed in more detail in [15], the decay dynamics of the signal generated depends, however, on the photon energy. This is shown in figure 9 where the dephasing time $T_2 = 2\tau_2$ as a function of the photon energy is given. In this case, the laser is tuned to the central photon energy of 3.199 eV and the photon energy of the detection is varied. The maximum intensity of excitation is quite high, namely 1.7 MW cm^{-2}. Inside the bottleneck region the dephasing time is almost constant while it decreases drastically outside the bottleneck region.

6. Discussion

We have studied the FWM signal dynamics in CuCl bulk material or epitaxial films in the bottleneck region in retrodiffusion and transmission configurations. As a function of time delay, the corresponding spectra show some similarities but also significant differences:

(i) In retrodiffusion, the signal maximum shifts to lower photon energies; in transmission its position is independent of the time delay.
(ii) Depending on the photon energy, the signals decay exponentially or double exponentially.
(iii) The observed time constants depend on the photon energy, the thickness of the sample, and on the measuring configuration.

In FWM discussed here, the signal decay is due to decrease of the polariton density in the region where the signal is generated and to the dephasing of the excitonic polaritons due to collision processes, which can result in a change of either their wavevector or their internal spin structure [15, 21]. As regards their dephasing processes in general, it is the exciton part of the polariton wavefunction which undergoes scattering processes [28] due to interactions with other quasiparticles or with crystal perturbations. At low intensities, excitonic polaritons mainly lose their phase, which is initially defined by the exciting light field, because of surface effects, scattering with impurities or imperfections, and through collisions with acoustic or optical phonons. Since the energy of longitudinal optical phonons in CuCl is 26 meV, scattering with optical phonons becomes significant only at higher temperature [15]. At higher intensities, exciton–exciton or exciton–carrier scattering processes may become important [29–31]. As stated above, due to the high binding energy of excitons and biexcitons in CuCl and the important spin–orbit splitting, only excitons of the Z_3-series are created, even when using spectrally broad femtosecond pulses. All other electronic quasiparticle populations can be neglected. Due to the high linear absorption, the excitation depth (in which also the signal is generated in a reflection configuration) is of the order of 10 nm. At our highest excitation intensities, this leads to exciton densities of about $N_{ex} = 10^{17}$ cm^{-3} for all the samples. Although the exciton Bohr radius of 0.7 nm is very small in CuCl, these densities are quite important and dephasing due to exciton–exciton scattering cannot be excluded *a priori*.

In the polariton dispersion relation, the different dephasing processes give rise to an energy-dependent damping spectrum $\Gamma(E)$ which influences the transmission and reflection spectra of semiconductors close to the excitonic resonances. Polariton scattering processes [32] and resulting damping spectra have been discussed in, amongst others, references [33–38], measuring simultaneously the reflection and transmission of thin CdS samples. Direct measurements of polariton dephasing were determined in CuCl by a combination of nondegenerate FWM and time-of-flight measurement [16]. As a general feature it turned out for CdS that the damping inside and below the exciton bottleneck is mainly determined by extrinsic polariton scattering processes (for example by elastic scattering with defects or impurities). In this region, the dephasing mainly follows the frequency behaviour of the

polariton group velocity. Above the exciton resonance, the dephasing increases resonantly as the inverse of the group velocity. In this region (above the longitudinal exciton) the dephasing is mainly due to a relaxation of upper-branch polaritons to states on the lower branch by emission of acoustical phonons. The situation can be even more complicated inside the bottleneck region due to the presence of non-dipole-active excitons, which couple to the polaritons due to residual symmetry-breaking interaction [38]. In CuCl, a resonance-enhanced damping was observed beyond the exciton resonance, which was attributed to polariton–polariton scattering [16]. These measurements were, in contrast to ours, performed with nondegenerate picosecond pulses, but the technique could not give definite results inside the bottleneck region because of the high reabsorption of the signal.

Let us now discuss the results of our measurements. In order to explain the fact that the spectra of the signal depend on the time delay in retrodiffusion but not in transmission, we have to recall the polariton nature of the excited quasiparticles. At temporal coincidence, the signal is maximal at 3.207 eV because the density of polariton states is maximal in this energy region. In the reflection configuration, since the sample is highly absorbing at the exciton resonance, the signal is generated mainly in a thin surface layer of the film. Polaritons, which undergo scattering processes or propagate out of this layer into the sample, are lost for the FWM process. Since polaritons at an energy $E = 3.202$ eV have the minimum group velocity (which is smaller by a factor of 4 than that of the ones close to 3.207 eV [27]), they stay during a longer time close to the surface and contribute to the FWM signal at longer delays. This leads to the spectral shift of the FWM with increasing time delay and to the different spectral shape when compared to the transmission configuration: if the signal is studied in transmission, reabsorption is equally important if the signal is generated at the front surface or in the bulk of the sample. The signal generation therefore does not depend on the polariton group velocity and the spectrum does not evolve with time delay.

When comparing figures 7, 3, and 4(*d*), measured for the same sample but in different configurations, we observe a similar initial rapid decrease, which dominates up to 500 fs. The second decrease shows a much longer time constant in transmission than in the reflection configuration. We tentatively explain the rapid-decay part as resulting from a parametric FWM process similar to the induced decay of biexcitons: unbound two-polariton states are excited by one beam through two-photon absorption and the other beam induces their recombination. Such a FWM process is resonantly enhanced at the exciton resonance and may show a very short time constant. A two-polariton state can change its internal spin structure through scattering with phonons or defects and thus lose its coherence. We attribute the decay of the FWM signal (figures 4(*a*), (*c*), and (*d*)) with the time constant $\tau_1 \approx 130$ fs as being mainly related to this effect. As shown in figure 6, the corresponding dephasing rates differ significantly from one film to the other, indicating the extrinsic nature of this relaxation process. This fast decay is absent in the platelet when studied at a photon energy of 3.195 eV (figure 4(*b*)), where only the slow exponential decay is observed. In the framework of the interpretation given above, this is due to the fact that at this photon energy the generation of a two-polariton state followed by an induced decay cannot take place with energy and momentum conservation.

As regards the long time constant, we attribute it to the coherence time of the polaritons. While a signal generated in transmission is sensitive to the different polariton dephasing processes only, one generated in retrodiffusion is also affected by surface-enhanced recombination and, as explained above, by the propagation of polaritons out of the excited region. The latter lead to a decrease of the time constant τ_2, but this is not due to a dephasing process.

It is interesting to notice that the FWM decay curves in figures 4(*a*) and (mainly) 7 show a slight modulation when compared to the double-exponential fit. Such a modulation

Table 1. Dephasing rates and decay times for different samples at $T = 5$ K.

Sample	Γ_0 (meV)	τ_2 (ps)
Platelet at 3.203 eV	1.10 ± 0.02	0.60 ± 0.01
Platelet at 3.195 eV	1.64 ± 0.02	0.40 ± 0.01
Film, 3 μm, 3.202 eV	1.70 ± 0.05	0.38 ± 0.02
Film, 0.1 μm, 3.202 eV	1.37 ± 0.02	0.48 ± 0.01
Film, 0.1 μm (in transmission) 3.202 eV	0.61 ± 0.03	1.08 ± 0.05

is clearly absent in figure 4(*b*). Although the structures are comparable to the noise level, they appear systematically and could be due to beating structures: close to the surface, bulk and surface polaritons are constructed from the same exciton wavefunctions. For wavevectors inside the bottleneck region, the dispersion of the surface polaritons is very close to that of longitudinal excitons. Therefore, the dispersions of the two types of polariton are parallel to each other. In a FWM experiment, both types of quasiparticle can be excited by the light beams since, due to the grating configuration, the in-plane wavevector of the polaritons is no longer conserved [22, 32]. This situation would lead to quantum beats in the FWM intensity inside the bottleneck region. The energy separation of 5.5 meV between the states (corresponding to the nonanalytical exchange interaction) leads to a beating period of 750 fs. This value is close to the periodicity in figures 4(*a*) and 7. Outside the bottleneck region, when measuring as in figure 4(*b*) at 3.195 eV, the energy separation would be 13 meV. This would correspond to a much faster beating period, which, in addition, would strongly depend on the photon energy and the beating structure would be washed out.

The dephasing rates $\Gamma_0 = \hbar/\tau_2$ of the samples studied are listed in table 1. One finds in retrodiffusion $\tau_2 = 0.6$–0.38 ps. These values are characteristic for the samples close to their surfaces and depend on the photon energy of the polaritons. They indicate that the platelet and the sample of 0.1 μm thickness have better surface qualities than the one with 3 μm thickness. This is probably due to the fact that the lattice mismatch between substrate and film leads to strain, which relaxes with increasing thickness and gives rise to a great number of defects. This hypothesis is supported by the fact that, when studying the substrate/CuCl interface for both films by FWM in reflection, we find longer time constants ($\tau_2 \sim 0.4$–0.6 ps), comparable to that of the platelet.

If one compares the result for τ_2 measured in transmission and reflection for the film of 0.1 μm thickness, one sees that the surface effects diminish τ_2 from its bulk value by a factor of 2.25. Since polaritons show a free polarization decay, one may deduce from the longer time constants τ_2 of the FWM signal in transmission the dephasing times of the polaritons $T_2 = 2\tau_2$. Therefore, one would expect T_2 for a bulk sample of good quality to take the value of 2.7 ps at its maximum and then depend on the photon energy, similarly to the case for the 0.1 μm film indicated in figure 9. For the 0.1 μm thick sample studied in transmission, one would deduce from table 1 a value of $T_2 = 2.16$ ps, which is quite comparable to the one postulated for the bulk sample. Since the polariton–acoustic phonon scattering is far too small in CuCl to explain these high damping values [16], we think that they are limited by extrinsic scattering effects.

As regards the insets of figures 3 and 9, we relate the decrease of the decay time τ_2 (increase of the dephasing rate) outside the bottleneck region to elastic scattering of the polaritons: in classical collision theory, the dephasing rate due to elastic scattering is given by $\Gamma_0 = N\sigma v_g$ where σ is the elastic scattering cross section, N the number of scattering centres, and v_g the group velocity of the quasiparticles. Like the density of states, v_g is strongly modified due to the polariton effect and increases rapidly outside the bottleneck region.

7. Conclusions

Dephasing times of excitonic polaritons in high-quality CuCl samples at 5 K have been evaluated from FWM experiments to the maximum value of $T_2 = 2.7$ ps inside the bottleneck region. Outside this region but close to the excitonic resonance frequencies, polaritons dephase much faster due to their increasing group velocity, which is important in elastic scattering processes. These values are much smaller than those reported in [16], which vary between 15 and 100 ps, depending on the photon energy. They are determined for photon energies outside the polariton bottleneck region where the samples are transparent. They are also smaller than but comparable with values inside the bottleneck region, which can be estimated from hyper-Raman scattering [23, 33]. They show linewidths (FWHM) of 0.2 meV (corresponding to a dephasing time $T_2 = 6.5$ ps). Since hyper-Raman scattering, even when measured at low intensities of excitation, is often connected to stimulated emission, such a line-shape analysis is not very precise and only leads to an estimate of the upper limit of the coherence time.

In thin films or bulk samples studied in reflection, surface recombination and polariton propagation shorten the signal decay time and give rise to an apparent dephasing time of $T_2 = 1.2$ ps. In addition, in different films, depending on their crystalline quality, an even faster decay of the FWM signals can be observed. It is of extrinsic character, i.e. it is due to additional surface recombination and scattering with impurities and/or imperfections.

Acknowledgments

The authors gratefully acknowledge many helpful discussions with R Lévy and the sample preparation by M Joucla, J L Loison, and G Versini. JK acknowledges financial support by the MENRT of France and DB by the 'Landesgraduiertenförderung' of the 'Land Baden-Württemberg' (Germany), the French Foreign Ministry, and the 'Région Alsace' (France). Financial support by the French Government MENRT–PECO-CEI (N/Ref 212802L) is gratefully acknowledged by EV. This work was partially supported by the Lithuanian State Science and Studies Foundation.

References

[1] Gilliot P, Moniatte J, Crégut O and Lévy R 1997 *Phys. Status Solidi* a **164** 441
[2] Braun W, Bayer M, Forchel A, Schmitt O M, Bányai L, Haug H and Filin A I 1998 *Phys. Rev.* B **57** 12 364
[3] Wagner H P, Langbein W, Hvam J M, Bacher G, Kümmell T and Forchel A 1998 *Phys. Rev.* B **57** 1797
[4] Wagner H P, Schätz A, Maier R, Langbein W and Hvam J M 1997 *Phys. Rev.* B **56** 12 581
[5] Wagner H P, Schätz A, Maier R, Langbein W and Hvam J M 1998 *Phys. Rev.* B **57** 1791
[6] Brinkmann D, Kudrna J, Gilliot P, Hönerlage B, Arnoult A, Cibert J and Tatarenko S 1999 *Phys. Rev.* B **60** 4474
[7] Gilliot P, Brinkmann D, Kudrna J, Crégut O, Lévy R, Arnoult A, Cibert J and Tatarenko S 1999 *Phys. Rev.* B **60** 5797
[8] Koch M, Plessen G V, Feldmann J and Göbel E O 1996 *Chem. Phys.* **120** 367
[9] Schultheis L, Kuhl J, Honold A and Tu C W 1986 *Phys. Rev. Lett.* **57** 1635
[10] Schultheis L, Kuhl J, Honold A and Tu C W 1986 *Phys. Rev. Lett.* **57** 1797
[11] Schwab H and Klingshirn C 1992 *Phys. Rev.* B **45** 6938
[12] Pantke K H and Hvam J M 1994 *J. Mod. Phys.* B **8** 73
[13] Dörnfeld C and Hvam J M 1989 *IEEE J. Quantum Electron.* **25** 905
[14] Gomes M J M, Kippelen B, Lévy R, Grun J B and Hönerlage B 1990 *Phys. Status Solidi* b **159** 101
[15] Vanagas E, Kudrna J, Brinkmann D, Gilliot P and Hönerlage B 2001 *Phys. Rev.* B **63** 153201
[16] Masumoto Y, Shionoya S and Takagahara T 1983 *Phys. Rev. Lett.* **51** 923
[17] Fröhlich D, Kulik A, Uebbing B, Mysyrowicz A, Langer V, Stotz H and von der Osten W 1991 *Phys. Rev. Lett.* **67** 2343
[18] Rossi F 1998 *Semicond. Sci. Technol.* **13** 147

[19] Nüsse S, Haring Bolivar P, Kurz H, Levy F, Chevy A and Lang O 1997 *Phys. Rev.* B **55** 4620
[20] Wundke K, Neukirch U, Kubacki F, Gutowski J and Hommel D 1996 *J. Cryst. Growth* **159** 800
[21] Hönerlage B, Lévy R, Grun J B, Klingshirn C and Bohnert K 1985 *Phys. Rep.* **124** 161
[22] Lagois J and Fischer B 1982 Surface polaritons *Modern Problems in Condensed Matter Sciences* vol 1, ed V M Agranovich and D L Mills (Amsterdam: North-Holland) p 69
[23] Hönerlage B, Bivas A and Vu Duy Phach 1978 *Phys. Rev. Lett.* **41** 49
[24] Vu Duy Phach, Bivas A, Hönerlage B and Grun J B 1977 *Phys. Status Solidi* b **84** 731
[25] Grun J B, Hönerlage B and Lévy R 1982 *Excitons* ed E I Rashba and M D Sturge (Amsterdam: North-Holland) p 459
[26] Göbel A, Ruf T, Lin Ch-T, Cardona M, Merle J-C and Joucla M 1997 *Phys. Rev.* B **56** 210
[27] Masumoto Y, Unuma Y, Tanaka Y and Shionoya S 1979 *J. Photogr. Sci.* **47** 1844
[28] Hopfield J J 1958 *Phys. Rev.* **112** 1555
[29] Klingshirn C and Haug H 1985 *Phys. Rep.* **70** 61
[30] Hönerlage B, Klingshirn C and Grun J B 1976 *Phys. Status Solidi* b **78** 599
[31] Benoit à la Guillaume C, Debever J M and Salvan F 1969 *Phys. Rev.* **177** 567
[32] Hopfield J J 1969 *Phys. Rev.* **182** 945
[33] Broser I, Pantke K-H and Rosenzweig M 1985 *Phys. Status Solidi* **132** K117
[34] Broser I, Pantke K-H and Rosenzweig M 1986 *Phys. Status Solidi* **138** K31
[35] Gourdon C and Lavallard P 1986 *Phys. Status Solidi* **138** K29
[36] Dagenais M and Sharfin W F F 1987 *Phys. Rev. Lett.* **58** 1776
[37] Pantke K-H and Broser I 1988 *J. Lumin.* **40, 41** 499
[38] Reznichenko V Ya, Strashnikova M I and Cherny V V 1991 *Phys. Status Solidi* **167** 311
[39] Lagois J and Fischer B 1978 *Advances in Solid State Physics* vol 18, ed J Treusch (New York: Academic) p 197
[40] Itoh T and Suzuki T 1978 *J. Photogr. Sci.* **45** 1939